Research Article/Araştırma Makalesi

GAZİ
JOURNAL OF ENGINEERING SCIENCES

Experimental Investigation of Dry Environment Abrasive Wear Behavior of a Plain Bearing Material

Recep Demirsöz[*a]

Submitted: 29.11.2021 Revised : 09.03.2022 Accepted: 09.03.2022 doi:10.30855/gmbd.2022.01.08

ABSTRACT

In this study, using variables such as load and sliding speed, which are effective parameters on abrasive wear, the amount of wear on the bearing material, friction coefficients, and trace depth values according to the experimental conditions were determined. According to the results of the analysis of variance performed as a result of the experiments carried out in the ball-on-flat experimental setup, the most effective parameter for all outputs was the load value, and the effect ratio for mass loss was 66.26%, the effect ratio for the friction coefficient was 53.02% and the effect ratio for the trace depth was 85.69%. The R^2 values obtained from the comparison of the experimental results with the regression results were found to be 0.9750, 0.9988, and 0.9759 for mass loss, friction coefficient, and trace depth, respectively. These results show that the regression model fit is good.

Keywords: Abrasive wear, dry sliding, bearing material, ANOVA

[a] Karabuk University, Faculty of Engineering, Dept. of Mechanical Engineering 78050 - Karabük, Türkiye
Orcid: 0000-0003-0674-4572

[*]Corresponding author: recepdemirsoz@karabuk.edu.tr

Bir Kaymalı Yatak Malzemesinin Kuru Ortam Abrazif Aşınma Davranışının Deneysel Olarak İncelenmesi

ÖZ

Bu çalışmada, abrazif aşınma konusunda etkili parametreler olan yük ve kayma hızı gibi değişkenler kullanılarak yatak malzemesinde meydana gelen aşınma miktarları, deney şartlarına göre sürtünme katsayıları ve iz derinliği değerleri belirlenmiştir. Ball-on-flat deney düzeneğinde gerçekleştirilen deneyler sonucunda yapılan varyans analizi sonuçlarına göre tüm çıktılar için en etkili parametre yük değeri olup kütle kaybı için etki oranı %66.26, sürtünme katsayısı için etki oranı %53.02 ve iz derinliği için etki oranı ise %85.69olarak bulunmuştur. Deneysel sonuçların regresyon sonuçları ile mukayesesinden elde edilen R^2 değerleri ise kütle kaybı, sürtünme katsayısı ve iz derinliği için sırası ile 0.9750, 0.9988 ve 0.9759 olarak bulunmuştur. Bu sonuçlar regresyon model uyumunun iyi olduğunu göstermektedir.

Anahtar Kelimeler: Abrazif aşınma, kuru sürtünme, yatak malzemesi, ANOVA metodu

To cite this article: R. Demirsöz, "Experimental Investigation of Dry Environment Abrasive Wear Behavior of a Plain Bearing Material," *Gazi Journal of Engineering Sciences,* vol.8, no.1, pp. 89-102, 2022. doi:10.30855/gmbd.2022.01.08

1. Introduction

The reason for many damages encountered in the industry is that the equipment is left without oil due to malfunctions of the lubrication systems. Lubrication is an indispensable requirement for almost all mechanical equipment. It is important that the amount of oil required by the rolling and sliding bearings used in the bearing of the rotating equipment is sent regularly and in sufficient quantities. Most of the time, this equipment can be left without oil for various reasons and therefore can be damaged in a short time. Since the roller bearings move according to the rolling method, they can tolerate this oil-free situation for a certain period. However, if the plain bearings are left without oil, that is, either no oil film is formed or the existing oil film is torn, metal-to-metal friction occurs.

In many previous studies, different wear environments were studied. There are studies on the environments, which are expressed as colloidal environments and contain particles in nanometer size that cannot be seen with the naked eye [1,2]. In their studies, Çetin and Korkmaz conducted experiments in a ball-on-flat experimental setup in a total of six different environments: dry environment, water environment, ethylene glycol and a medium containing three different nano-silver ratios of 4%-8% and 12%, respectively [3]. two different speeds and two different load values were chosen in the experiments. According to the results, it was concluded that with the increase in the number of nano-silver particles, a 33.99% reduction in mass loss, an improvement of 21.13% in surface quality, an 18.16% decrease in friction coefficient and a 74.31% decrease in ambient temperature were achieved. Leon et al. boronized AISI 316L stainless steel material was subjected to dry friction test in a ball-on-flat experimental setup [4]. They selected load, distance, sliding speed and distance as variables. As a result of the experiments, they got the results of wear rate, scar depth and friction coefficient as output. They carried out their experiments according to ASTM G133-05 standard procedures and on the UMT-2 universal test setup. As a result of the statistical analyses they performed on the results, it was revealed that the load variable had an effect of 63.7%, 59.60% and 62.67% on the wear rate, scar depth and friction coefficient, respectively. Sudhakar et al. In their study, they studied the effects of alloying elements on the dry friction performance of high chromium white cast iron and Ni-hard iron materials [5]. Vanadium, titanium and boron elements were used for high chromium white cast iron material as alloying element. The wear tests were carried out on a pin-on disc test setup at 159 rpm, 319 rpm and 478 rpm, and at 10-20 and 30 N load values. They concluded that the highest wear rate was reached when the medium speed of 319 rpm and the highest load value of 30 N were applied. It was observed that the wear rate decreased as the sliding speed increased from 159 rpm to 478 rpm at a lower load value of 10 N. In this case it was mainly due to the lubricity of the matrix. It was observed that the friction coefficient decreased with the increase of the rotational speed. For all alloys, it was determined that it was the highest at 159 rpm and the lowest at 478 rpm.

In their study, Elleuch et al. carried out dry friction wear tests on a pin-on-disc experimental setup using CW614 bronze material [6]. They used 52100 steel as an abrasive. They used 20, 40 and 80 N load and 1, 4 and 7 m/s velocity values as variables. They chose 3500m as the friction distance. They evaluated the chemical composition, surface morphology and microstructure of the worn surface by performing SEM (Scanning Electron Microscope) imaging and EDX (Energy Dispersive X-Ray) measurements on the wear surfaces. They concluded that the coefficient of friction in dry friction directly affects the temperature increase in the contact zone.

In their study, Mindivan et al. used a synchronizer ring made of high strength (α+β) bronze material. [7] They studied the wear behavior of this material in the dry friction state in the pin-on-disc assembly. It was determined that the increase of the α phase in the microstructure of the synchronizer rings from 8% to 23% by volume decreased the hardness value from 281 to 250HV but increased the wear resistance of the material. They concluded that, depending on the type of test and the counter surface, the increase in wear resistance of the synchronizers ranged from 15% to 80%.

In this current study, the wear behavior of the plain bearing material of monoblock stands used in Wire Rod Mills around the world in dry friction condition was investigated. Ball-on-flat experimental setup was used in this experimental study. Copper alloy material was used as the bearing material and 100Cr6 bearing steel with a diameter of 6mm was used as the abrasive. The experiments were carried out at three different sliding speeds, 10 rpm, 30 rpm and 50 rpm, and at three different loads, 10 N, 20 N and 30 N. The mentioned parameters were chosen in the light of preliminary experiments and close to the values in the literature [8,9]. Wear values were measured as mass loss in mg, and wear was

analysed visually and elementally using SEM, EDX. Analysis of Variance (ANOVA) method was used for the statistical analysis of the test results and mass loss, friction coefficient and surface roughness measurements were made. As a result of the study, it has been revealed that load change is a parameter that is approximately three times more effective than speed change in dry friction.

2. Materials and Method

2.1. Preparation of specimens

The chemical composition of the bearing material is given in Table 1. The specimens used were prepared in the dimensions of 30 mm x 30 mm and were connected to the specimen slot in the experimental setup by using the clamping apparatus. The specimens were grounded by SiC emery paper before the experiments. In Figure 1, the SEM view surface of the grounded specimen is given. In Table 2, the hardness of the bearing material and the average surface roughness values before and after sanding are given. Values were taken from three different points on the specimen.

Table 1. Chemical composition of bronze bearing material

Element	Cu	Sn	Ni	Pb	Zn	Al	Mn	Fe	Others
[wt%]	86.88	1.45	3.63	3.68	0.00	0.22	0.41	0.44	3.29

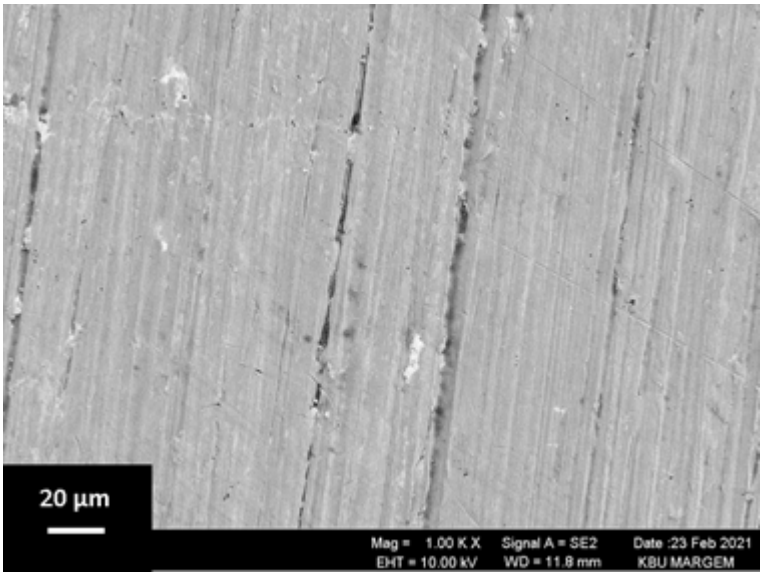

Figure 1. SEM image of the surface sanded with SiC emery paper

Table 2. Hardness and surface roughness values of bearing material

Measured surface hardness value [HV]	Surface roughness before sanding, Ra [µm]	Surface roughness after sanding, Ra [µm]
60.9 ±0.67	2.268 ±0.685	0.274 ±0.022

2.2. Abrasive wear tests

The wear tests of the bearing material were carried out by using the Ball-on-flat test apparatus on the two-functional test equipment containing the Pin-on-disc and Ball-on-flat apparatuses, which are visualized in Figure 2. The rotational movement obtained from an electric motor on the said mechanism is converted into a linear movement with the help of the mechanism it is connected to. The stroke length is 13 mm, and this value gives the length of the traces obtained on the specimen surfaces. The rotational speed of the mentioned electric motor can be changed with a drive system in order to obtain the desired abrasive speed. There is a load arm that balances at no load on the assembly, allowing the position of the abrasive ball to be adjusted depending on the specimen thickness. While adjusting, the horizontal position of the arm can be controlled with the help of a spirit level. There is a chamber (pot) that can be used to create a liquid medium for placing the specimen to be abraded. The experiments were carried out at room temperature and no significant temperature increase was observed in the specimen during the preliminary experiments.

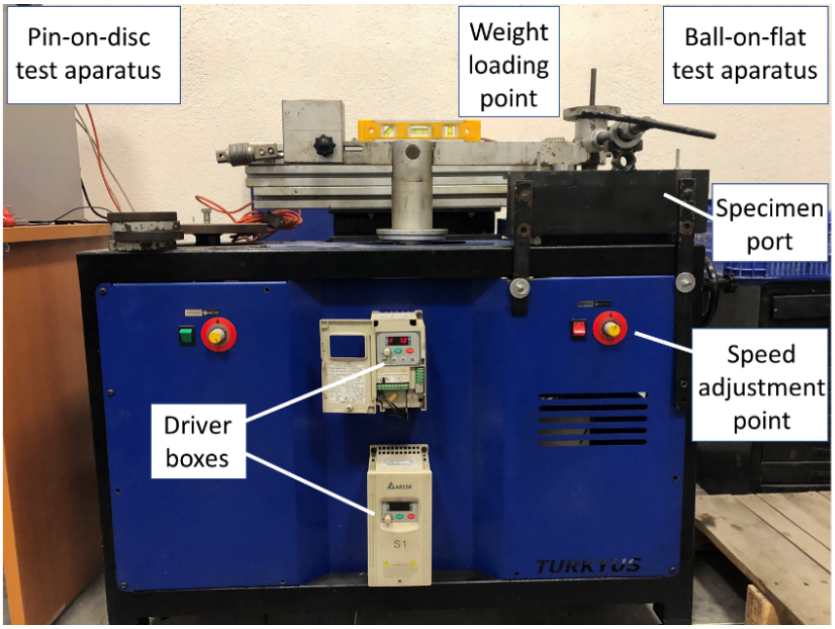

Figure 2. Ball-on-flat test rig

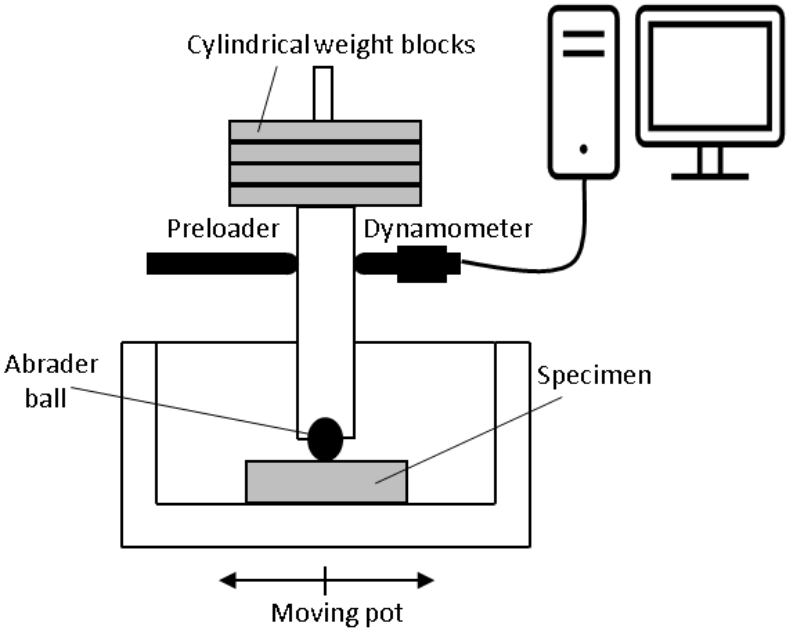

Figure 3. Schematic image of the experimental setup

As an abrasive, 100Cr6 (AISI 52100-64HRC) ball material with 6 mm diameter spherical geometry was used in order to be resistant to test specimens [3,10-13]. After each experiment, the ball was changed, and the new experiment was started with a new abrasive ball. The chemical composition of the abrasive ball obtained by EDX is given in Table 3. According to the preliminary experiments, three different load values as 10 N, 20 N, and 30 N and three different rotational speed values of 10 rpm, 30 rpm, and 50 rpm were determined in the experiments to be carried out. The sliding speed values corresponding to the number of revolutions are given in Table 4. The experiments were carried out in 9 different experimental conditions according to the full factorial experimental design (3 load x 3 speed) and these test parameters are given in Table 5. Three replications were made for each experimental condition. After the experiments, the specimens were cleaned using compressor air set to 7 bar in order to remove the wear residues and not affect the weighing results. Before weighing, it was dried for 3 minutes with the help of a blow dryer in order to remove possible moisture from the compressor. After all these processes, mass losses were measured with a DENSI brand HZY 320 A model precision balance with a weighing sensitivity of 0.1 mg.

Table 3. Chemical composition of the 100Cr6 abrader ball

Element	C	Mn	P	S	Si	Ni	Cr	Cu
wt%	0.95	0.35	0.025	0.015	0.25	0.30	1.55	0.3

Table 4. Speed parameters conversion table

Rotational Speed [rpm]	Sliding Speed [mm/s]
10	8.66
30	26.00
50	43.33

Table 5. Parameters used in the experiments

Exp. No	Load [N]	Rotational Speed [rpm]	Sliding Distance [m]
1	10	10	
2	10	30	
3	10	50	
4	20	10	
5	20	30	100
6	20	50	
7	30	10	
8	30	30	
9	30	50	

2.3. Statistical Analysis

This experimental study was carried out as full factorial. Nine (3*3) experiments were carried out using three different loads and three different speeds. Experiments were repeated three times for each condition. As a result of the experiments, three different outputs were obtained, namely mass loss, friction coefficient and trace depth. In order to quantitatively determine the effects of input variables on output variables and to see the effects of input parameters on output values, full quadratic ANOVA was performed on the experimental results. ANOVA (Analysis of Variance) is a method used to determine possible relationships and relationship strengths between inputs and outputs [14]. Analysis values revealed which input variable was effective on the results for system optimization. Equations were obtained by using the Response Surface Method (RSM) according to the mass loss, friction coefficient and trace depth results. In addition, R-Square values were obtained by comparing the experimental results and the estimated results obtained from the modeling. The R-Sq value is an indicator of whether the experiments were successful or unsuccessful. It can be stated that the experimental significance of wear is 70% and above, and the results are sufficient for the R-Sq value obtained. Minitab software program was used in all analysis procedures [3]. While performing the statistical analysis, the 95% confidence interval was taken into account [15] In this statistical method, the statistical and physical importance is the p value, the order of importance is the F value, and the effect of the input parameters on the output parameters is the % effect value [16]. P value less than or equal to 0.05 indicates that physical and statistically significant results occur [17].

3. Results and Discussions

3.1. Mass Loss

Mass losses, friction coefficients, and trace depths were measured at different load and speed values used in the experiments. The mass loss, friction coefficient, and trace depth values obtained as a result of three different tests for each test condition are given in Table 6.

The amount of mass loss according to the sliding speed and load values are given graphically in Figure 4. According to the obtained mass loss values, the lowest mass loss value of 3.3 mg was obtained under 10 N load and 8.66 mm/s sliding speed conditions. The highest value was 21.3 mg, and the highest load value was 30 N and the highest speed value was 43.33 mm/s.

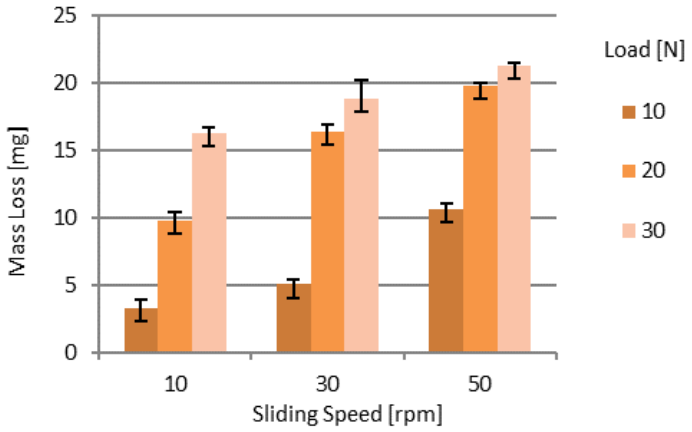

Figure 4. Mass loss values obtained from the wear

Table 6. Mass loss, friction coefficient, and trace depth values

Exp. No	Load [N]	Sliding Speed [rpm]	Mass Loss [mg]	Friction Coefficient	Trace Depth [µm]
1	10	10	3.3 ±0.624	0.446 ±0.012	43.63 ±6.1
2	10	30	5.1 ±0.300	0.435 ±0.006	58.17 ±2.6
3	10	50	10.7 ±0.361	0.411±0.012	91.80 ±9.1
4	20	10	9.8 ±0.608	0.435±0.016	90.3 ±5.0
5	20	30	16.4 ±0.557	0.421±0.028	127.67 ±7.6
6	20	50	19.8 ±0.265	0.395±0.011	132.00 ±2.6
7	30	10	16.3 ±0.458	0.541±0.002	191.67 ±11.0
8	30	30	18.9 ±1.353	0.514±0.035	211.00 ±8.5
9	30	50	21.3 ±0.265	0.485±0.013	260.33 ±3.8

According to the ANOVA, the effect rate of the load parameter, which is the most effective parameter in dry friction conditions, on the results was found to be 66.261% (Table 7). As the load increases, the mass loss also increases.

The same can be said for speed. The 2.495% error value obtained as a result of the analysis can be said to be caused by the vibration and material microstructure that has not been taken into account [3]. The effect rate of the second variable, the speed parameter, was found to be 24.447%. In addition, equation (1) was obtained for mass loss calculation with the RSM. The R^2 value was calculated based on the experimental results and the values from the regression calculation, and this value was found to be 0.975 and is given in Figure 5. High value indicates good regression model fit.

Table 7. ANOVA analysis table for mass loss

Source	Degree of Freedom (DoF)	Sum of Square (SS)	Mean Square (MS)	F-Value	P-Value	Parameter Contribution Rate [%]
A - Load [N]	1	226.66	226.66	79.67	0.003	66.261
B - Speed [rpm]	1	83.627	83.627	29.4	0.012	24.447
AxA	1	14.942	14.942	5.25	0.106	4.368
BxB	1	1.472	1.472	0.52	0.524	0.430
AxB	1	1.83	1.83	0.64	0.481	0.535
Error	3	8.535	2.845			2.495
Total	8	342.069				100.000

$$Mass\ Loss\ (ML)[mg] = -16.70 + 1.811xA + 0.392xB - 0.0273xA^2 - 0.00231xB^2 - 0.00335xAxB \quad (1)$$

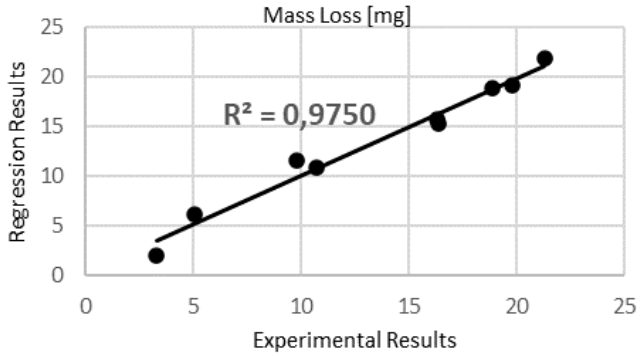

Figure 5. Comparison of experimental results and RSM values for the mass loss

3.2. Coefficient of friction

ANOVA shows that the most effective parameter for friction coefficient values is the load parameter, and the effect rate on the results was found to be 53.021%, as seen in Table 8. The 0.14% error value obtained because of the analysis, on the other hand, can be said to occur due to unconsidered parameters like the mass loss [3]. The effect rate of the second variable, the speed parameter, was found to be 14.793%. In addition, equation (2) was obtained for the coefficient of friction calculation with the RSM. The R^2 value was calculated based on the experimental results and the values from the regression calculation, and this value was found to be 0.9988 and is given graphically in Figure 7. A high value indicates good regression model fit.

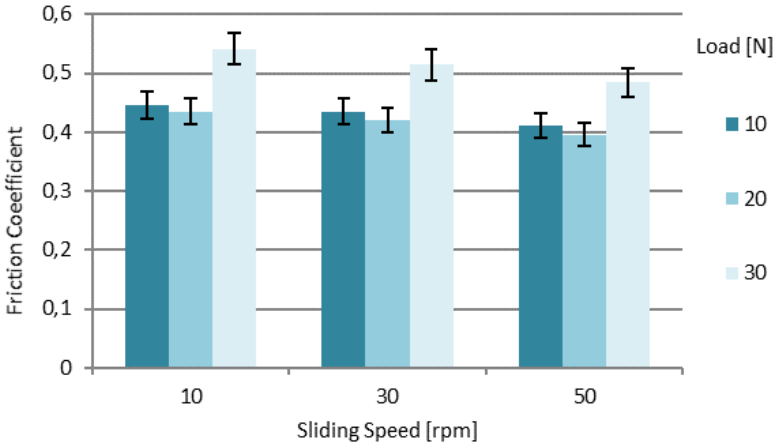

Figure 6. Friction coefficient values obtained from the wear tests

$$Coefficient\ of\ Friction\ (CoF) = 0.56421 - 0.017079xA + 0.000108xB + 0.000550xA^2 - 0.000011xB^2 - 0.000026xAxB \quad (2)$$

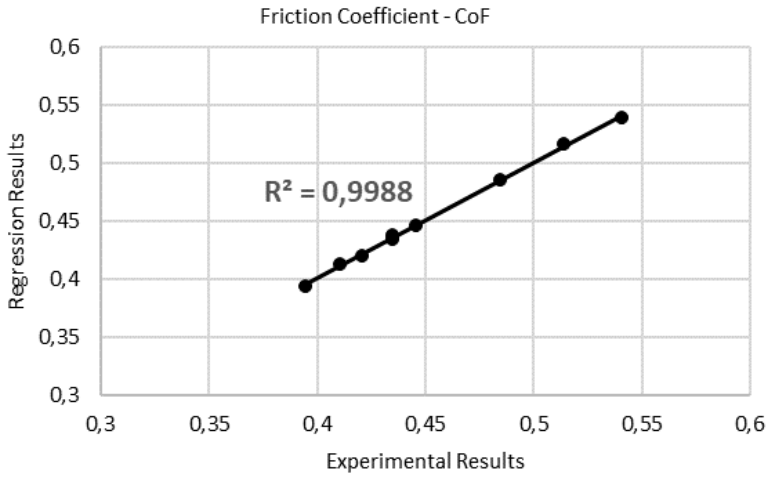

Figure 7. Comparison of experimental results and RSM values for the coefficient of friction

3.3. Inspection of wear profiles and surfaces

In this study, the wear mechanisms on the surfaces were investigated using the ZEISS ULTRA PLUS scanning electron microscope, which is shown in Figure 8a. EDX analyses were performed to determine the wear mechanisms on the surface. The surface roughness values obtained as a result of the specimen preparation processes before the experiment were measured in the Mitutuyo SJ-410 model surface roughness measuring device, whose image is given in Figure 8b, and trace forms (Figure 9) were obtained with the help of the same device. The sampling numbers were chosen as 3 for surface roughness measurements and for wear trace form determinations.

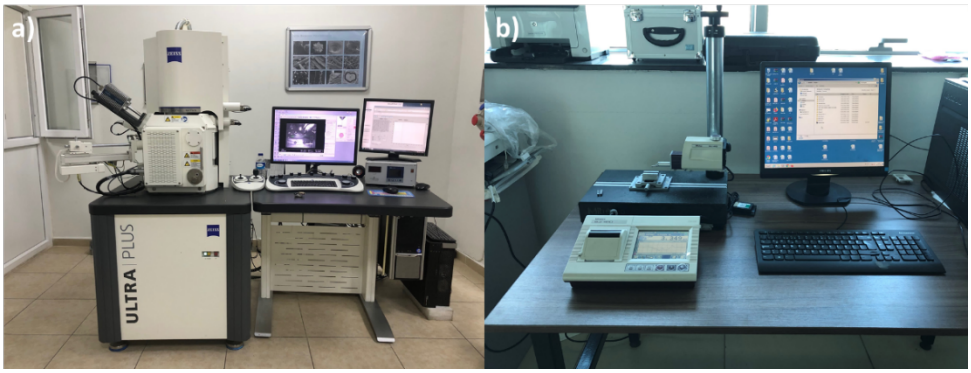

Figure 8. (a) SEM device image, (b) Roughness measuring device image

Table 8. ANOVA analysis table for coefficient of friction

Source	Degree of Freedom (DoF)	Sum of Square (SS)	Mean Square (MS)	F-Value	P-Value	Parameter Contribution Rate [%]
A - Load [N]	1	0.010251	0.010251	1371.84	0.00004	53.021
B - Speed [rpm]	1	0.00286	0.00286	382.77	0.00029	14.793
AxA	1	0.00605	0.00605	809.67	0.0001	31.292
BxB	1	0.00004	0.00004	5.42	0.10232	0.207
AxB	1	0.00011	0.00011	14.75	0.03112	0.569
Error	3	0.000022	0.000007			0.114
Total	8	0.019334				100.000

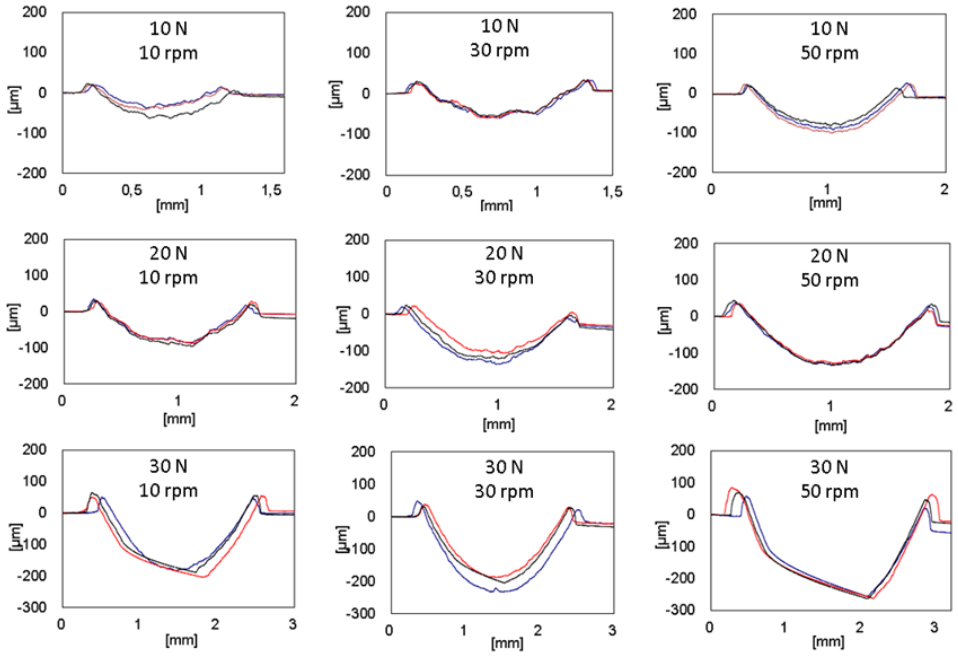

Figure 9. Trace profiles resulting from wear

ANOVA shows that the most effective parameter for trace depth values is the load parameter, as in other outputs. As can be seen from Table 9, it was found to be 85.688%. As a result of the analysis, an error value of 1.086% was found. The effect rate of the second variable, the speed parameter, was found to be 9.760%. Equation (3) was obtained for the trace depth calculation. R^2 value was calculated using experimental results and estimation values and this value was found as 0.9891. R^2 graph is given in Figure 11. According to this graph, it was concluded that the regression model fit was good.

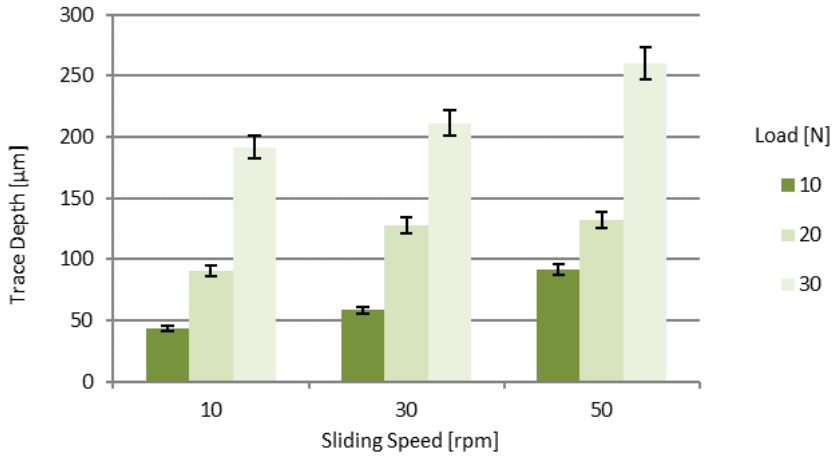

Figure 10. Trace depth values obtained from the wear tests

Table 9. ANOVA analysis table for trace depth

Source	Degree of Freedom (DoF)	Sum of Square (SS)	Mean Square (MS)	F-Value	P-Value	Parameter Contribution Rate [%]
A - Load [N]	1	36774.9	36774.9	236.72	0.001	85.688
B - Speed [rpm]	1	4188.8	4188.8	26.96	0.014	9.760
AxA	1	1369.4	1369.4	8.81	0.059	3.191
BxB	1	13.2	13.2	0.08	0.079	0.031
AxB	1	105.1	105.1	0.68	0.471	0.245
Error	3	466	155.3			1.086
Total	8	42917.4				100.000

$$Trace\ Depth\ (TD)[\mu m] = 44.5 - 3.41xA + 0.42xB + 0.2617xA^2 + 0.0064xB^2 - 0.0256xAxB \quad (3)$$

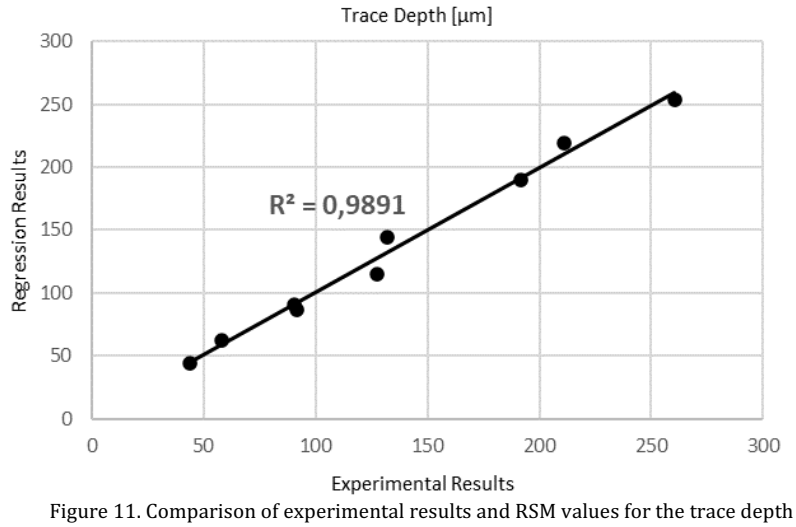

Figure 11. Comparison of experimental results and RSM values for the trace depth

SEM images were examined to determine the wear mechanisms on the surfaces. SEM images of the wear profiles obtained from the experiments carried out with all load and speed variables are given in Figure 12, respectively. As can be seen from the SEM images, the mass loss and the trace depth values are compatible with each other. When the results obtained are examined, the parameters with the highest wear and trace depth values are 30 N load and 50 rpm values. The wear mechanisms of the surface obtained as a result of this experiment are shown on SEM images in Figures 13 and 14. No excessive deformation was observed in most parts of the surface on the wearing surfaces. Uniformly eroded areas were also found on the wear surface. In the EDX micro-analyses, particles that broke off from the abrasive sphere and penetrated the material surface were found. The fact that the Cr element was found in the investigated area is the biggest indicator of this. Also, in EDX micro-analysis, particles penetrated to the surface were also found on the material surface. Ploughing marks on the surface are not very deep and are present in many parts of the surface. In places, delamination and large amounts of material smearing were also observed. Particularly in areas where material agglomeration occurs, interlayer embedded particles were found. There are also furrows in the areas close to the material agglomerations. Although not extremely deep, there are also pitting areas. When the trace profiles are examined, it is seen that there is a more indented structure in the profiles at low load values. As the load value increases, the roughness of the profiles decreases. The same can be said for low-speed values. Profile roughness decreases at high-speed values.

Table 10. List of surface defects detected in SEM images

Abbreviations	Type of wear mechanism
ABP	Abrasive ball particle
SPD	Severe particle deformation
EP	Embedded particle
PL	Ploughing
MA	Material agglomeration
S	Smearing
P	Pitting
F	Furrows
D	Delamination

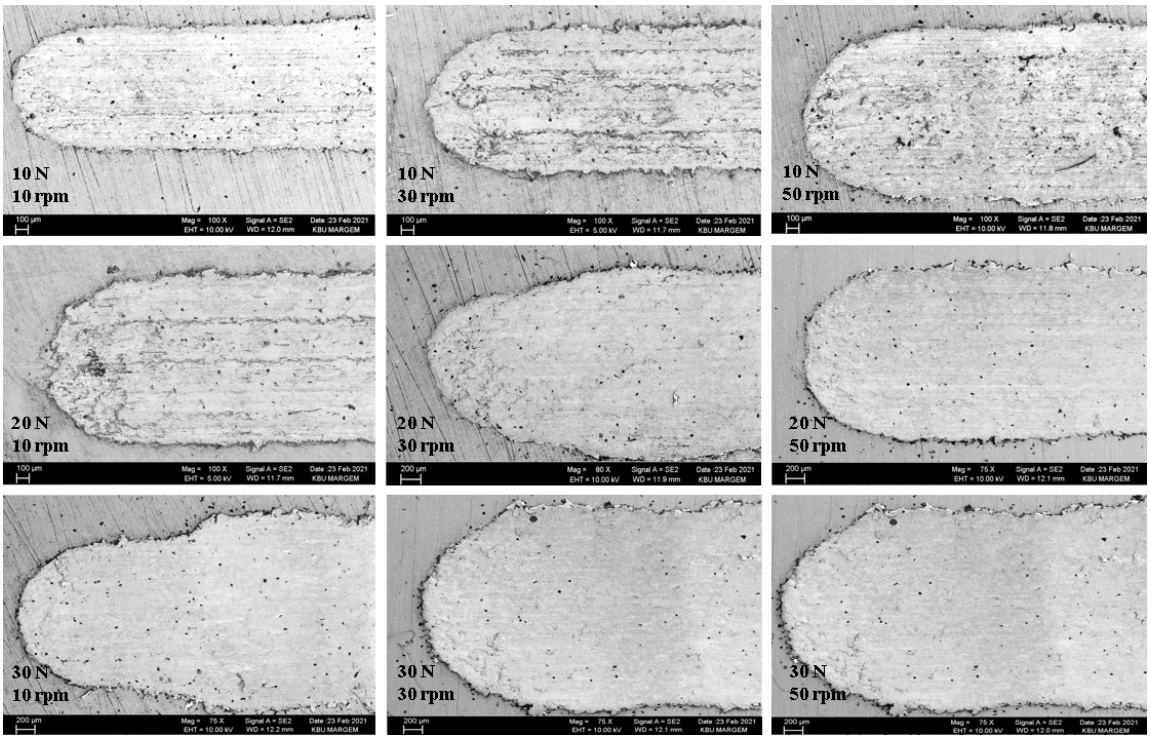

Figure 12. SEM images of the worn surface

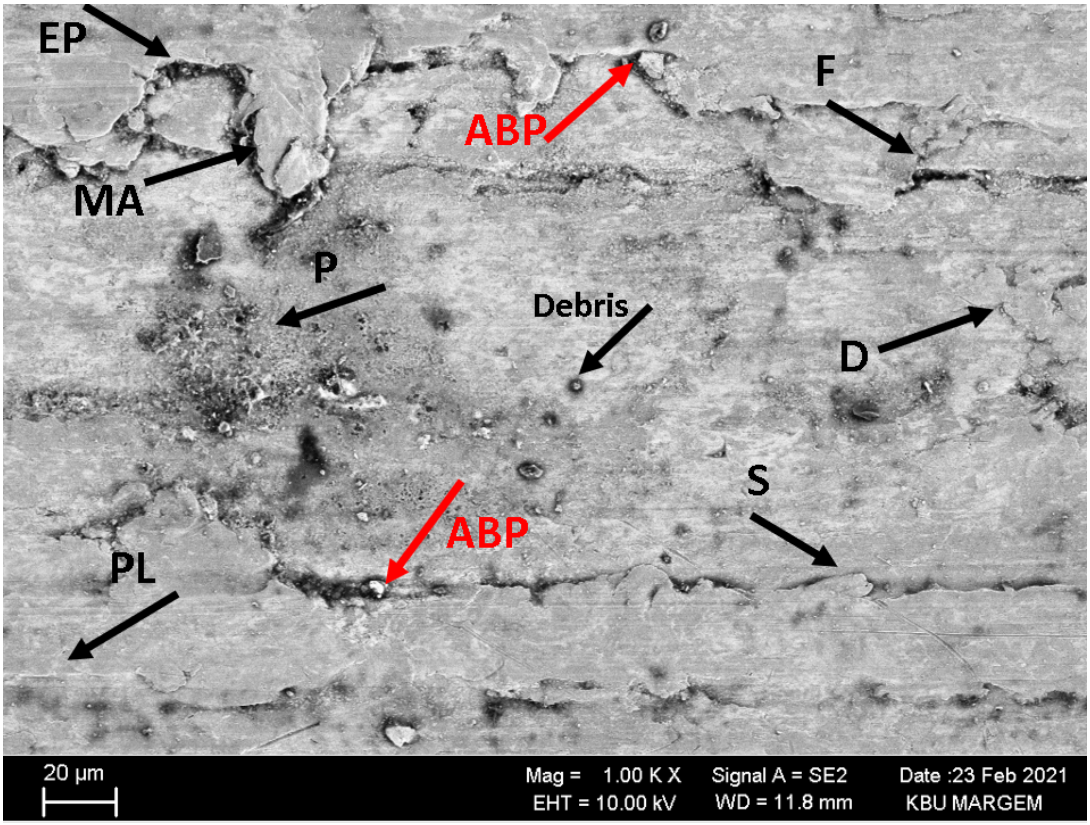

Figure 13. SEM image of material exposed to wear at 30 N load and 50 rpm sliding speed

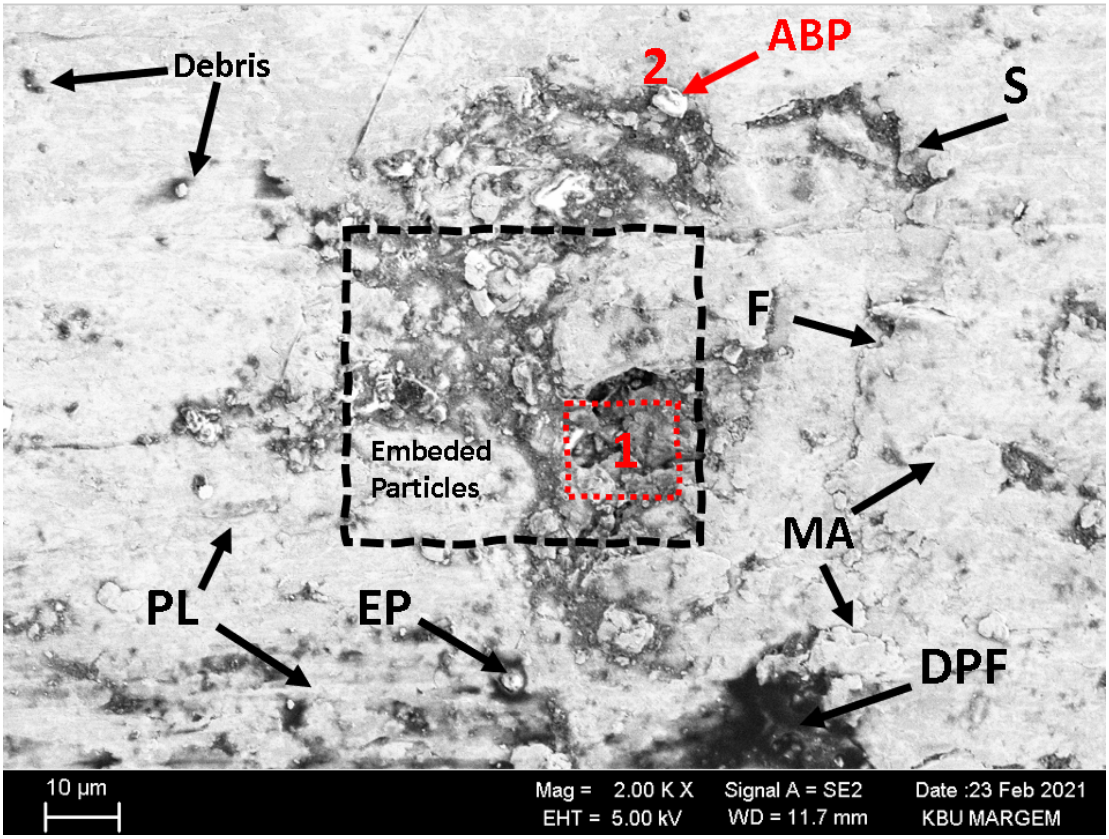

Figure 14. SEM image of material exposed to wear at 30 N load and 50 rpm sliding speed

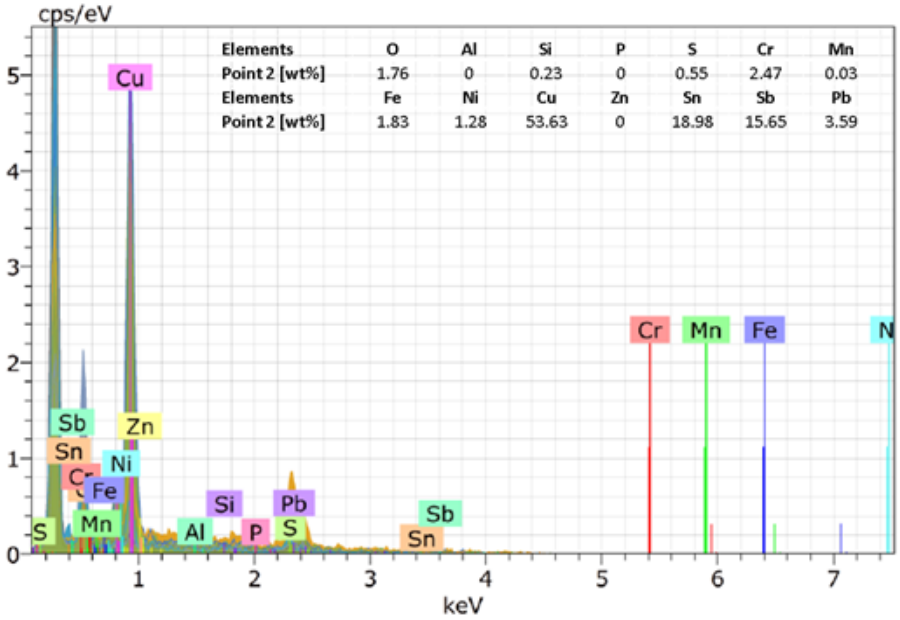

Figure 15. EDX micro analysis values of Point 2 on Figure 14

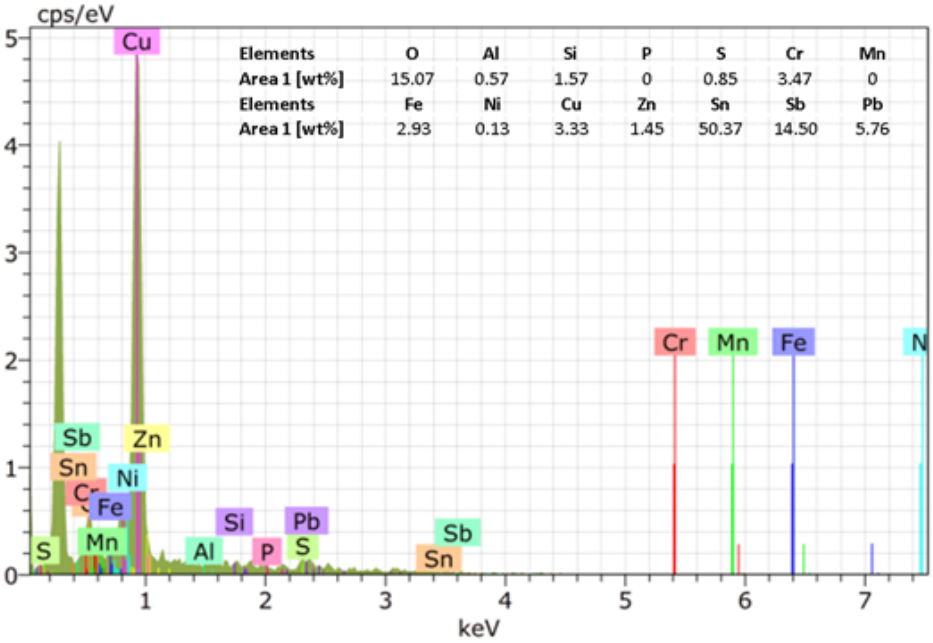

Figure 16. EDX micro analysis values of Area 1 on Figure 14

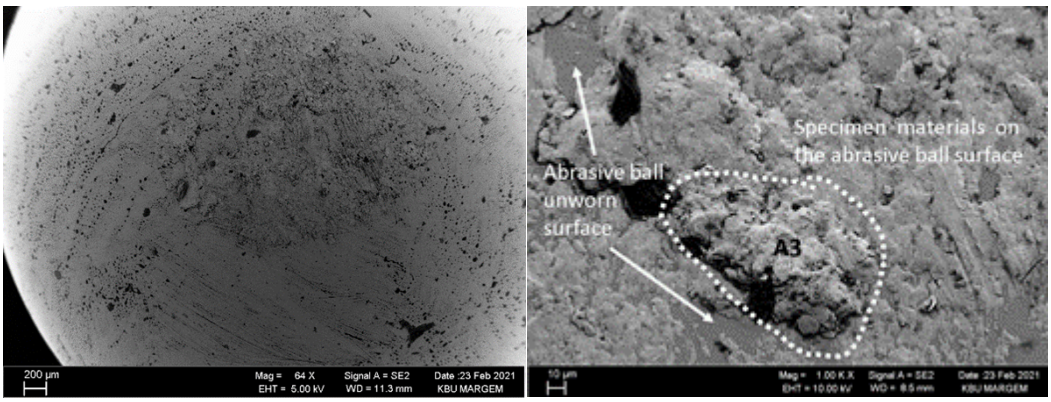

Figure 17. SEM images of the abrasive ball surface

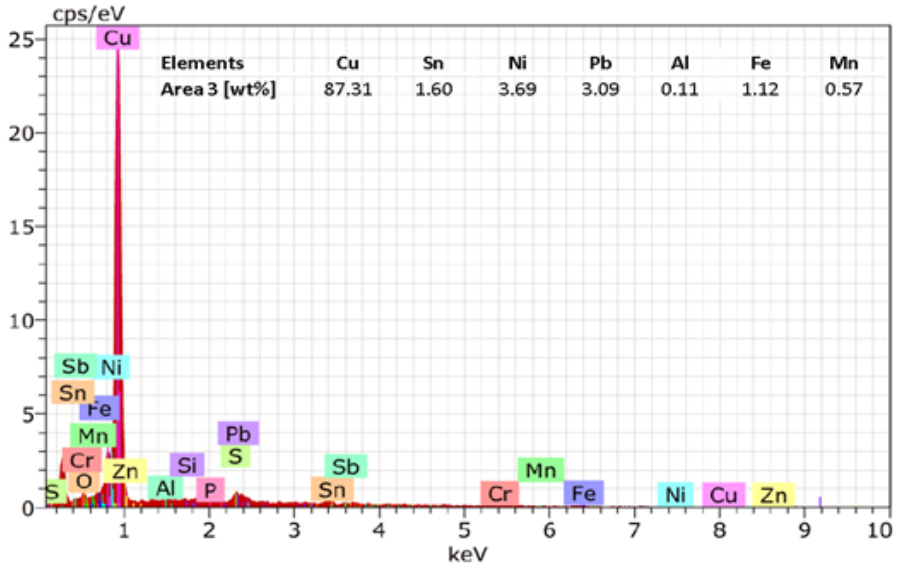

Figure 18. EDX micro analysis values of Area 3 on Figure 17

3. Conclusions

In this study, the bronze bearing material used as a plain bearing was subjected to dry sliding at different load and speed values. As a result of the experiments, results such as mass loss, friction and trace depth were obtained, and these results were analysed. Experimental results were analysed using the ANOVA method. In addition, SEM and EDX images were taken from the specimen's surfaces and evaluations were made on the surface wear. It can be evaluated in terms of the results obtained.

1. It can be clearly said that the independent variable effective on mass loss in dry friction conditions is load. The effect rate of the load on the wear was determined as 66.261%. In addition, the effect of the load decreases after 20 N. The effect rate of the speed is 24.447% and the wear effect increases with the increase in speed, but this change is linear. According to the ANOVA results, it can be said that the effects of the load and speed variables are significant since the P value is less than 0.05. However, since the squares and interaction values of the variables are greater than 0.05, it can be said that they do not have statistical effects. The R^2 value between the mass loss values calculated using the model formula obtained with RSM and the experimental results was 0.975, and the high value of this value indicates that the regression model fit is good.

2. Again, the load is the effective variable in determining the friction coefficient. This rate was determined as 53.021%. The friction coefficient value of 20 N, which is the intermediate value for each speed value in the change of load, has been determined as the smallest values. It can be said that the load and speed variables are significant according to the ANOVA results. It can be said that it is statistically insignificant only because the effect of the square of the velocity value is greater than 0.05. The R^2 value between the friction coefficient values obtained because of the model calculation and the experimental results was found to be 0.9988, and it is seen that the regression model fit is good.

3. The results obtained for the trace depth showed that the load variable was quite effective. There is an impact rate of 85.688%. It can be said that the trace depth results are essentially parallel to the mass loss values. The effect of the load change increases after 20 N, unlike the mass loss. As a result of ANOVA, although the load and velocity values are statistically effective, they are statistically ineffective because the squares of the variables and the interaction value are greater than 0.05. In the regression analysis, the R^2 value was found to be 0.9759, and the regression model fit was quite good.

4. The load variable emerged as the most effective parameter on the mass loss, friction coefficient and trace depth values because of the experiments performed on the ball-on-flat experimental setup, and these values were determined as 66.261%, 53.021% and 85.688%, respectively.

By using the models obtained in the light of the analysis revealed in this study, parameters can be selected to obtain appropriate friction coefficient and low wear values without experimental studies.

Acknowledgment

This study was supported by Karabük University Scientific Research Projects with Project number of KBÜBAP-21-ABP-062.

Conflict of Interest Statement

The authors declare that there is no conflict of interest

References

[1] E. De Robertis, E.H.H. Cosme, R.S. Neves, A.Y. Kuznetsov, A.P.C. Campos and S.M. Landi, "Application of the modulated temperature differential scanning calorimetry technique for the determination of the specific heat of copper nanofluids," *Applied Thermal Engineering,* vol. 41, pp. 10–17, 2012. doi:10.1016/j.applthermaleng.2012.01.003.

[2] S. M. S. Murshed, "Determination of effective specific heat of nanofluids," *Journal of Experimental Nanoscience*, vol. 6 no. 5, pp. 539–546, 2011. doi:10.1080/17458080.2010.498838.

[3] M. H. Cetin and S. Korkmaz, "Investigation of the concentration rate and aggregation behaviour of nano-silver added colloidal suspensions on wear behaviour of metallic materials by using ANOVA method," *Tribology International*, vol. 147, pp. 106273, 2020. doi:10.1016/j.triboint.2020.106273.

[4] R. A. García-León, J. Martínez-Trinidad, R. Zepeda-Bautista, I. Campos-Silva, A. Guevara-Morales, J. Martínez-Londoño and J. Barbosa-Saldaña, "Dry sliding wear test on borided AISI 316L stainless steel under ball-on-flat configuration: A statistical analysis," *Tribology International*, vol. 157, 2021. doi:10.1016/j.triboint.2021.106885.

[5] A. N. Sudhakar, R. Markandeya, B. Srinivasa Rao, Ajoy Kumar Pandey and D. Kaushik, "Effect of alloying elements on the dry sliding wear behavior of high chromium white cast iron and Ni-hard iron," *Materials Today: Proceedings*, 2021. doi:10.1016/j.matpr.2021.09.295.

[6] Elleuch, Khaled, Riadh Elleuch, Ridha Mnif, Vincent Fridrici, and Philippe Kapsa, "Sliding Wear Transition for the CW614 Brass Alloy," *Tribology International* vol. 39 no. 4, pp. 290–96, 2006. doi:10.1016/j.triboint.2005.01.036.

[7] Mindivan, H., H. Çimenoğlu, and E. S. Kayali, "Microstructures and Wear Properties of Brass Synchroniser Rings," *Wear* vol. 254, no. 5–6, pp. 532–37, 2003. doi:10.1016/S0043-1648(03)00023-1.

[8] L. Xu, Y. Zhang, D. Zhang and M. Leng, "Preparation and tribological properties of Ag nanoparticles/reduced graphene oxide nanocomposites," *Industrial Lubrication and Tribology*, vol. 70, pp. 1684–1691, 2017. doi:10.1108/ILT-03-2017-0054.

[9] G. Pitchayyapillai, P. Seenikannan, P. Balasundar and P. Narayanasamy, "Effect of nanosilver on microstructure, mechanical and tribological properties of cast 6061 aluminum alloy," *Transactions of Nonferrous Metals Society of China,* vol. 27, pp. 2137–2145, 2017. doi:10.1016/S1003-6326(17)60239-5.

[10] H. Ghaednia, M.S. Hossain and R.L. Jackson, "Tribological Performance of Silver Nanoparticle–Enhanced Polyethylene Glycol Lubricants," *Tribology Transactions,* vol. 59, pp. 585–592, 2016. doi:10.1080/10402004.2015.1092623.

[11] L. Gara and Q. Zou, "Friction and wear characteristics of oil-based ZnO nanofluids," *Tribology Transactions,* vol. 56, pp. 236–244, 2013. doi:10.1080/10402004.2012.740148.

[12] H. Xie, B. Jiang, J. He, X. Xia and F. Pan, "Lubrication performance of MoS2 and SiO_2 nanoparticles as lubricant additives in magnesium alloy-steel contacts," *Tribology International,* vol. 93, pp. 63–70, 2016. doi: 10.1016/j.triboint.2015.08.009.

[13] Y. Y. Wu, W. C. Tsui and T. C. Liu, "Experimental analysis of tribological properties of lubricating oils with nanoparticle additives," *Wear*, vol. 262, pp. 819–825, 2007. doi: 10.1016/j.wear.2006.08.021.

[14] N. Yalçın, Y. Kayır ve S. Erkal, "AA2024 Alüminyum Alaşımına Uygulanan Yaşlandırma Yöntemlerinin İşlenebilirliğe Etkisinin Taguchi ve Anova ile Araştırılması," *Journal of Polytechnic*, cilt 20, sayı 4, ss. 743–51, 2017. doi:10.2339/politeknik.368552.

[15] E. Nas, E. Zurnacı ve S. Yıldırım, "Sertleştirilmiş AISI H13 Takım Çeliğinin Delme Performansını İyileştirmek İçin Elektro Erozyon İşleme Parametrelerinin Taguchi Yöntemi Kullanılarak Modellenmesi ve Optimizasyonu," *Gazi Journal of Engineering Sciences*, cilt 7, sayı 2, ss. 99–110, 2021. doi:10.30855/gmbd.2021.02.03.

[16] B. Özlü, M. Akgün ve H. Demir, "AA 6061 Alaşımının Tornalanmasında Kesme Parametrelerinin Yüzey Pürüzlülüğü Üzerine Etkisinin Analizi ve Optimizasyonu," *Gazi J. Eng. Sci.*, cilt 5, sayı 2, ss. 151–158, 2019. doi:10.30855/gmbd.2019.02.04.

[17] B. Kondul, "Borlama ile yüzeyi sertleştirilmiş ray çeliğinin aşınma davranışının incelenmesi," Yüksek Lisans Tezi, KBÜ, Karabük, Türkiye, 2020.